J. At. Mol. Sci.
doi: 10.4208/jams.090913.121413a

Vol. **5**, No. 2, pp. 178-186
May 2014

Theoretical study of the two-dimensional momentum spectra of H^- ion in the intense laser fields

Chang-Ping Sun[a]*and Bao-Feng Cui[b]

[a] *School of Science and Institute of Condensed Matter Physics, Linyi University, Linyi 276000, China*
[b] *Experimental Management Center, Linyi University, Linyi 276000, China*

Received 9 September 2013; Accepted (in revised version) 14 December 2013
Published Online 28 February 2014

Abstract. By using two model potentials chosen, the second outermost back rescattered ridges (BRR) of the two-dimensional (2D) momentum spectra of H^- ion in the linear polarization laser fields are studied under the strong-field approximation (SFA). The results show that the polarization potentials in the two model potentials have little effect on the 2D momentum spectra, the number of BRR increases and the fluctuation of angular distributions along the second BRR decreases with the increase of the laser intensity, but the accurate electron-atom elastic scattering cross sections can be retrieved directly along the second outermost BRR by the polynomial fitting method.

PACS: 32.80Gc, 42.50Hz

Key words: strong field approximation method, time-dependent Schrödinger equation, momentum spectra

1 Introduction

Strong field physics is an important frontier field in the present physics research [1, 2]. The above-threshold ionization (ATI) of atoms and molecules is the one of the most fundamental processes of the interaction between intense laser fields and atoms and molecules, which can provide urgently needed data and theoretical support for the new particle accelerator [3, 4], attosecond physics [5, 6] and atomic structure measurements [7, 8], etc. The study of ATI of atoms and molecules in the intense laser fields can not only further understand the laser properties, but also has important significance for understanding the interaction mechanism between atoms and molecules and intense laser

*Corresponding author. *Email address:* sunchangping8011@163.com (C. P. Sun)

fields. In recent decades, the momentum and energy spectra of the negative ions in intense laser fields had been extensively studied [9], where H^- ion was reported in experiments [10-12] and in theories [13-18].

Theoretically, the principal theoretical methods have the strong-field approximation (SFA) method and the numerical solution of time-dependent Schrödinger equation (TDSE) method. The TDSE method can obtain accurate results, but the defects of TDSE are large amount of calculation and limited to computer hardware and software. Since SFA method treats the continuum states with the Volkov states, and neglects that the nucleus has influence of Coulomb field on the ionization electrons, thus SFA method can be used to study the photodetachment of negative ions in intense laser fields quiet well [17, 18].

In recent years, the most back rescattered ridges (BRR) of the two-dimensional (2D) momentum spectra of neutral atoms [19-22] and negative ions [18] have been studied theoretically, but the study on the second outermost BRR of the 2D momentum spectra has not been reported. The recent study results show that the 2D photoelectron momentum spectra of H^- ion in the intense laser fields obtained using SFA method are in good agreement with the ones obtained using TDSE method [18]. To further study the second outermost BRR of the 2D photoelectron momentum spectra of H^- ion and the influence of static potential and polarization potential included model potentials on the 2D photoelectron momentum spectra in the different laser fields, the 2D photoelectron momentum spectra of H^- ion in the linear polarization laser fields are calculated using the SFA method by choosing two model potentials. Atomic units are used throughout the paper unless otherwise indicated.

2 Theoretical method

The detachment amplitude of H^- ion with momentum p is expressed as [23]

$$f(p)=f^{(1)}+f^{(2)}. \tag{1}$$

The first and second terms are, respectively, the first-order and second-order amplitude, and they can be expressed as

$$f^{(1)}=-i\int_{-\infty}^{+\infty}dt\langle\chi_p(t)|H_i(t)|\Psi_0(t)\rangle \tag{2}$$

$$f^{(2)}=-\int_{-infty}^{+\infty}dt\int_{-\infty}^{t}dt'\int dk\langle\chi_p(t)|V|\chi_k(t)\rangle\times\langle\chi_p(t')|H'(t')|\Psi_0(t')\rangle \tag{3}$$

where V, $\Psi_0(t)$ and $\chi_p(t)$ are model potential, initial wavefunction and Volkov state wavefunction with the momentum p, respectively.

In the linear polarization laser field, the 2D photoelectron momentum spectra can be expressed as

$$\frac{\partial^2 P}{\partial E\partial\theta}=|f(P)|^2 2\pi p\sin\theta. \tag{4}$$

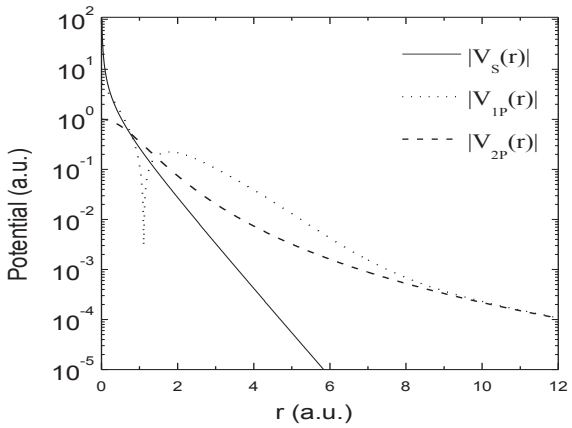

Figure 1: Schematic of the static potential and polarization potential in the model potentials $V_1(r)$ and $V_2(r)$ of H^- ion

The energy spectra is given by integrating the angle θ as

$$\frac{\partial P}{\partial E}=\int |f(P)|^2 2\pi p \sin\theta d\theta. \tag{5}$$

The initial wavefunction of H^- ion [24] can be expressed as

$$\Psi_{1s}(r)=0.75\exp(-0.235r)Y_{00}(\hat{r})/r \tag{6}$$

Two model potentials $V_1(r)$ [25] and $V_2(r)$ [24] chosen are expressed as

$$V_1(r)=V_S(r)+V_{1P}(r)=-(1+\frac{1}{r})e^{-2r}-\frac{\alpha_d}{2r^4}(1-e^{-(r/r_c)^6})+(c_0+c_1r+c_2r^2)e^{-\beta r}, \tag{7}$$

$$V_2(r)=V_S(r)+V_{2P}(r)=-(1+\frac{1}{r})e^{-2r}-\frac{\alpha_p}{2(r^2+d^2)^2}, \quad d^4=\frac{\alpha_p}{2Z^{1/3}} \tag{8}$$

The model potentials $V_1(r)$ and $V_2(r)$ include the same static potential and different polarization potentials, where the static potential $V_1(r)$ is $-(1+\frac{1}{r})e^{-2r}$, the polarization potential $V_{1P}(r)$ and $V_{2P}(r)$ are $-\frac{\alpha_d}{2r^4}(1-e^{-(r/r_c)^6})+(c_0+c_1r+c_2r^2)e^{-\beta r}$ and $-\frac{\alpha_p}{2(r^2+d^2)^2}$, respectively. The parameters in Eq. (7) and Eq. (8) are given in Ref. [25] and Ref. [24], respectively. Schematic of the static potential and polarization potential in the model potentials $V_1(r)$ and $V_2(r)$ are shown in Fig. 1.

3 Results and discussion

The linearly polarized electric field of the laser pulse along the z axis is given by

$$E(t)=E_0\alpha(t)\cos(\omega t+\phi) \tag{9}$$

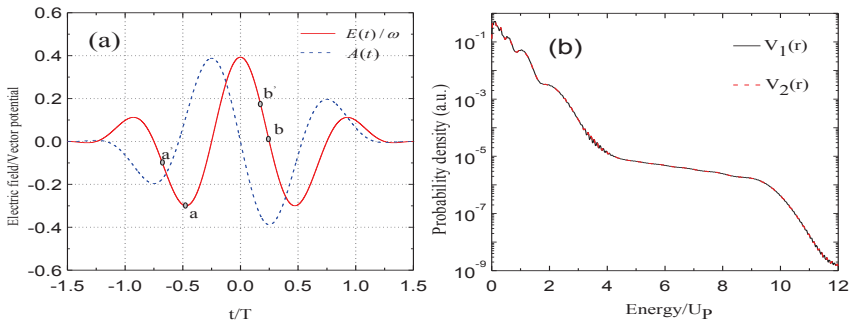

Figure 2: (a) Schematic of the laser electric $E(t)$ and the vector potential $A(t)$ of a three-cycle laser pulse, with $\lambda=10600$ nm and $I=1.0\times10^{11}$ W/cm^2; (b) Comparison of energy spectra of model potentials $V_1(r)$ and $V_2(r)$.

where $\alpha(t)=\cos^2(\pi t/\tau)$ is the envelope function, ω is the frequency of the pulse, E_0 is the amplitude, and ϕ is the carrier-envelope phase ($\phi=0$). The pulse duration $\tau=3T$ (T is the optical cycle of the laser pulse, $|t|\leq\tau/2$).

To study the second outermost BRR of the 2D photoelectron momentum spectra of H^- ion and the influence of the static potential and polarization potential included model potentials on the 2D photoelectron momentum spectra in the different laser fields, the 2D photoelectron momentum spectra of H^- in the linear polarization laser fields were calculated using the SFA method by using two model potentials. The electric field $E(t)=-\partial A(t)/\partial t$ and the vector potential $A(t)$ of such a laser pulse are depicted in Fig. 2(a). We chose a laser pulse with the wavelength of 10600 nm and peak intensity of 10^{11} W/cm^2. Fig. 2(b) shows the comparison of energy spectra of model potentials $V_1(r)$ and $V_2(r)$, we can clearly see that they agree quite well. Since the model potentials and are different only in the polarization (see in Fig. 1), thus the polarization potentials in the two model potentials have little influence on the energy spectra.

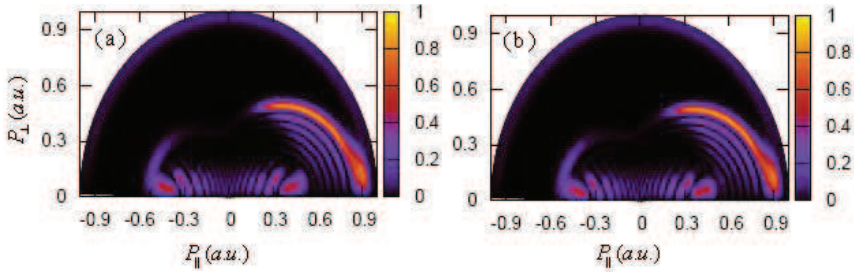

Figure 3: 2D photoelectron momentum spectra calculated with $V_1(r)$ model positional and $V_2(r)$ model positional. (a) The result of model positional $V_1(r)$; (b) The result of model positional $V_2(r)$. The laser parameters are the same as Fig. 2.

Fig. 3 shows the 2D photoelectron momentum spectra calculated with model positionals $V_1(r)$ and $V_2(r)$. Since the electron yield drops very rapidly with energy (see

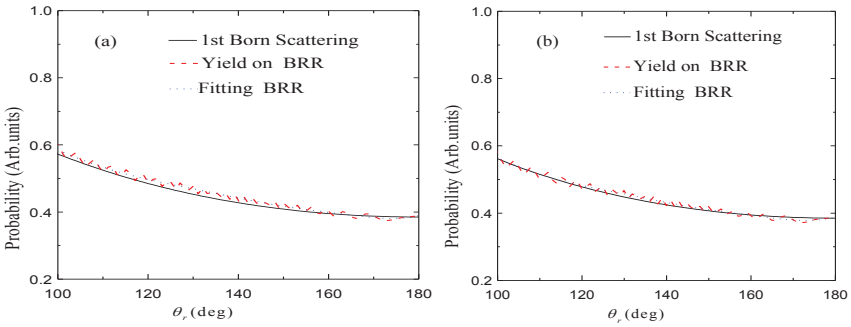

Figure 4: Angular distributions of photoelectrons along the second outermost BRR and the polynomial fitting results of them for H^- compared to the differential elastic scattering cross sections calculated using the FBA. Fig. 4 (a) and Fig. 4 (b) are the second outermost BRR along the Fig. 3(a) and Fig. 3(b), respectively.

Fig. 2(b)), to display the full electron momentum image surface in a single plot, the 2D momentum spectra in each frame have been renormalized such that the total ionization which yields at each electron energy is the same in Fig. 3. The horizontal axis $P_\square$ is along the direction of the laser's polarization and the vertical axis $P_\perp$ is along any direction perpendicular to it. From Fig. 3 we can extract that the 2D momentum spectra obtained from model potentials $V_1(r)$ and $V_2(r)$ are in good agreement, thus the polarization potentials in the two model potentials also have little influence on the momentum spectra. In Fig. 3 there are many half circular rings called back rescattered ridges (BRR) [19]. In this paper, the right-side BRR in Fig. 3 are named the outmost BRR, the second outmost BRR, the third outmost BRR, etc accordingly from right to left. The recent study results [18-22] show that the appearance cause of the right-side outmost BRR in Fig. 3 can get well explained with the schematic of the laser electric $E(t)$ and the vector potential $A(t)$ in Fig. 2(a), namely the appearance cause of the outmost BRR is that the BRR on the "right" in Fig. 2(a) is from electrons born at time near 11a", travelling to the right and then returning to the target ion at time near "b", where they are rescattered back to the right. The momentum of the outmost BRR electrons is given by $p = A_r + p_r$ or $p_\square = -A_r - p_r \cos\theta_r$, where A_r is the vector potential at "b", p_r is the radius of BRR, θ_r is the backscattering angle, ranging from 90° to 180°, and the relation between A_r and p_r is $p_r = 1.26A_r$ obtained by the classical theory calculation. To study the appearance cause of BRR, we studied the angular distributions of photoelectrons along the second outermost BRR in Fig. 3(a) and Fig. 3(b), where center position A_r is 0.351 and radius p_r is 0.439, which is in good agreement with $p_r = 0.442$ obtained from the classical theory formula $p_r = 1.26A_r$. The error between them is only 0.68%. Fig. 4(a) and Fig. 4(b) are the angular distributions of photoelectrons along the second outermost BRR and the polynomial fitting results of them for H^- ion compared to the differential elastic scattering cross sections calculated using the first Born approximation (FBA). Fig. 4(a) and Fig. 4(b) show that the calculation result of $V_1(r)$ agrees with the one of $V_2(r)$ quite well, the angular distributions of photoelectrons along the second outermost BRR have very fine wave character, but the

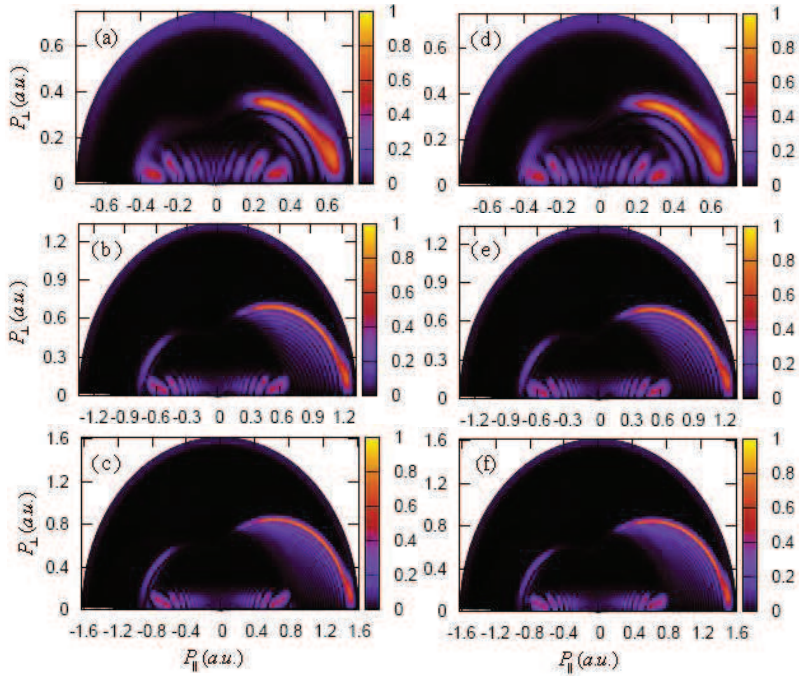

Figure 5: 2D photoelectron momentum spectra of H^- ion at the different laser intensities. Left column and right column are the calculation results of $V_1(r)$ and $V_2(r)$, respectively. From up to down, the laser intensities are, respectively, 0.5×10^{11}, 2.0×10^{11}, and 3.0×10^{11} W/cm^2.

Table 1: Comparison of the "measured" radius p_r as the center position A_r in the second outmost BRR of Fig. 6 with the p_r calculated by the classical theory formula.

Intensity (W/cm^2)	A_r(a.u.)	p_r(a.u.)	p_r calculated by the classical theory formula (a.u.)	Error (%)
5×10^{10}	0.234	0.291	0.295	1.36
1×10^{11}	0.351	0.439	0.442	0.68
2×10^{11}	0.515	0.645	0.649	0.62
3×10^{11}	0.636	0.805	0.801	0.50

polynomial fitting results are in good agreement with the ones calculated using the FBA. The appearance cause of the second outmost BRR is similar with the one of the outmost BRR, which can get well explained with the schematic of the laser electric $E(t)$ and the vector potential $A(t)$ in Fig. 2(a), namely the appearance cause of the outmost BRR is that the BRR on the "right" in Fig. 2(a) is from electrons born at time near "a'", travelling to the right and then returning to the target ion at time near "b'", where they are rescattered back to the right.

To study the 2D photoelectron momentum spectra of H^- ion in the intense laser

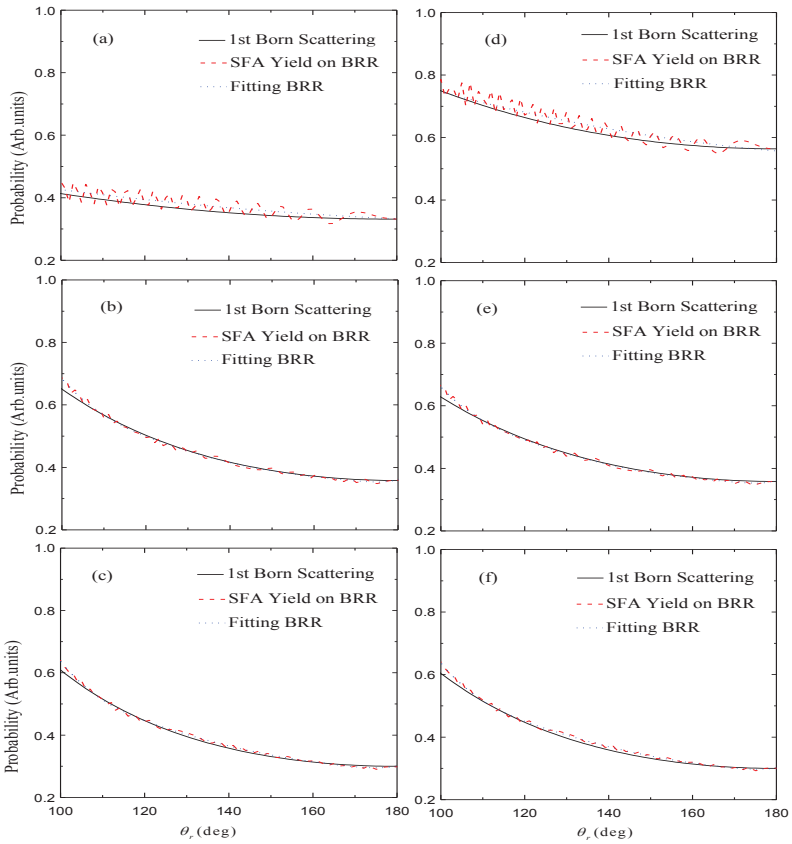

Figure 6: Angular distributions of photoelectrons along the second outermost BRR and the polynomial fitting results of them calculated using model potential $V_1(r)$ and $V_2(r)$ were compared to the differential elastic scattering cross sections calculated using the FBA. Left column and right column are the results of model potentials $V_1(r)$ and $V_2(r)$, respectively. Fig. 6 (a) - (c) and Fig. 6 (e) - (f) are the second outermost BRR along the Fig. 5 (a) - (c) and Fig. 5 (e) - (f), respectively.

fields with the wavelength of 10600 nm at the different laser intensities, we calculated the 2D photoelectron momentum spectra of H^- ion at the laser intensities , respectively, 0.5×10^{11}, 2.0×10^{11}, and 3.0×10^{11} W/cm^2 with the same model potentials $V_1(r)$ and $V_2(r)$ as the mentioned above. Fig. 5 shows the calculation results, where left column and right column are the calculation results of $V_1(r)$ and $V_2(r)$, respectively. From up to down, the laser intensities are, respectively, 0.5×10^{11}, 2.0×10^{11}, and 3.0×10^{11} W/cm^2. We can see from Fig. 5 that both of the calculation results obtained from these two model potentials are coincident each other perfectly well, the number of BRR increases with the increase of the laser intensity. To quantitatively study the appearance cause of the second BRR along the Fig. 5 (a) to (f), Fig. 6(a) to (f) show the angular distributions of photoelectrons along the second outermost BRR and the polynomial fitting results of them compared to the differential elastic scattering cross sections calculated using the FBA.

Fig. 6(a) to (f) show that the number of BRR increases and the fluctuation of angular distributions along the second BRR decreases with the increase of the laser intensity, but the accurate electron-atom elastic scattering cross sections can be retrieved directly along the second outermost BRR by the polynomial fitting method. The appearance cause of the above phenomena in Fig. 6(a) to (f) is because of the different collision probability between ionization photoelectrons of H^- ion and parent nucleus in the intense laser fields at the different intensities. To further test our calculation results, Table 1 shows that the "measured" radius p_r as the center position A_r in the second outmost BRR in Fig. 6 and compared the "measured" radius p_r with the calculation results by the classical theory formula $p_r = 1.26A_r$. From the Table 1 we can see that the "measured" the radius p_r are in good agreement with the classical calculation results, and the higher the laser intensity, the smaller the error is, where the maximal error of p_r is about 1.36% which comes from the laser pulse of intensity 5.0×10^{10} W/cm^2.

4 Conclusions

By using two model potentials $V_1(r)$ and $V_2(r)$ chosen, the second outermost BRR of the 2D momentum spectra of H^- ion in the linear polarization laser fields with the different intensities were studied using the SFA method. The results show that the polarization potentials in the two model potentials have little effect on the 2D momentum spectra, the number of BRR increases and the fluctuation of angular distributions along the second BRR decreases with the increase of the laser intensity, but the accurate electron-atom elastic scattering cross sections can be retrieved directly along the second outermost BRR by the polynomial fitting method, which is especially suitable for the case of the lower laser intensity. Compared with the numerical solution of TDSE, SFA method neglects the Coulomb attraction between the ionized electrons and their parent nucleus and the contribution of atomic excited states, but since the Coulomb interaction contributes little for the negative ions, thus SFA is an effective method for study detachment of negative ions in intense laser fields, and has many advantages, such as small computational amount, high calculation accuracy, clear physical processes, etc. Our results have certain reference value to study the above-threshold photodetachment of negative ions system in the intense laser fields.

Acknowledgments. This work was supported by the National Science Foundation of China (Grant Nos. 11247208 and 11064013) and Key Disciplines of Condensed Matter Physics of Linyi University.

References

[1] J. Zhang, Physics 26 (1997) 643. (in Chinese)
[2] T. Brabec and F. Krausz, Rev. Mod. Phys. 72 (2000) 545.
[3] C. I. Moore, A. Ting, S. J. McNaught, *et al.*, Phys. Rev. Lett. 82 (1999) 1688.

[4] Y. I. Salamin and F. H. M. Faisal, Phys. Rev. A 61 (2000) 043801.
[5] A. Baltuška, Th. Udem, M. Uiberacker, *et al.*, Nature 421 (2003) 611.
[6] G. Sansone, E. Benedetti, F. Calegari, *et al.*, Science 314 (2006) 443.
[7] M. Hentschel, R. Kienberger, C. Spielmann, *et al.*, Nature 414 (2001) 509.
[8] R. Kienberger, E. Goulielmakis, M. Uiberacker, *et al.*, Nature 427(2003) 817.
[9] F. Krausz and M. Ivanov, Rev. Mod. Phys. 81 (2009) 163.
[10] L. Præstegaard, T. Andersen, and P. Balling, Phys. Rev. A 59 (1999) R3154.
[11] R. Reichle, H. Helm, and I. Y. Kiyan, Phys. Rev. Lett. 87 (2001) 243001.
[12] X. M. Zhao, M. S. Gulley, H. C. Bryant, *et al.*, Phys. Rev. Lett. 78 (1997) 1656.
[13] C. Arendt, D. Dimitrovski, and J. S. Brigg, Phys. Rev. A 76 (2007) 023423.
[14] D. A. Telnov and S.-I. Chu, Phys. Rev. A 50 (1994) 4099.
[15] M. V. Frolov, N. L. Manakov, E. A. Pronin, *et al.*, Phys. Rev. Lett. 91 (2003) 053003.
[16] K. Krajewska, I. I. Fabrikant, and A. F. Starace, Phys. Rev. A 74 (2006) 053407.
[17] D. Bauer, D. B. Milosevic, and W. Becker, Phys. Rev. A 72 (2005) 023415.
[18] X. X. Zhou, Z. Chen, T. Morishita, *et al.*, Phys. Rev. A 77 (2008) 053410.
[19] Z. Chen, T. Morishita, A.-T. Le, *et al.*, Phys. Rev. A 76 (2007) 043402.
[20] T. Morishita, A.-T. Le, Z. Chen, *et al.*, Phys. Rev. Lett. 100 (2008) 013903.
[21] Z. Chen, A.-T. Le, T. Morishita, *et al.*, J. Phys. B 42 (2009) 061001.
[22] C. P. Sun, S. F. Zhao, J. H. Chen, *et al.*, Chinese Phys. B 20 (2011) 113201.
[23] W. Becker, F. Grasbon, R. Kopold, *et al.*, Adv. At. Mol. Opt. Phys. 48 (2002) 35.
[24] A. Gazibegović-Busuladžić, D. B. Milošević, and W. Becker, Phys. Rev. A 70 (2004) 053403.
[25] C. Laughlin and S.-I. Chu, Phys. Rev. A 48 (1993) 4654.